
Article:
Daood, S.S., Yelland, T.S., Szuhanszki, J. et al. (2 more authors) (2019) Experimental investigation of NO reburning during oxy-coal burner staging. Energy and Fuels, 33 (2). pp. 1590-1602. ISSN 0887-0624

https://doi.org/10.1021/acs.energyfuels.8b03823

Experimental investigation of NO reburning during oxy-coal burner staging

*Syed Sheraz Daood *, Thomas S. Yelland, János Szuhánszki, Mohamed Pourkashanian, William Nimmo*

Energy 2050, Energy Engineering Group, Department of Mechanical Engineering, University of Sheffield, Sheffield, S10 2TN, United Kingdom.

KEYWORDS

Oxy-coal combustion, NOx, burner staging, stoichiometry

ABSTRACT

This study presents an investigation into the impact of varied burner staging environments on an oxy-fuel flame and the rate of the NO formation and destruction processes. The experimental data was extracted from the use of a 250 kW_{th} down-fired combustion test facility with a scaled-down model of an industrial low-NO_x burner (LNB). Two oxy-coal combustion regimes were investigated by varying a fixed flow of oxidant between the secondary and tertiary registers, so as to impact the stoichiometry in the fuel-rich region and flame structure, and using various NO recycling regimes, to test the impact of these different burner configurations on NO reburning. The data was collected by monitoring key emissions in the flue gas and in the flame, as well as temperatures throughout the furnace and the unburned carbon content of the ash. A detailed investigation encompassing the impact of secondary oxidant proportion for different oxidants on NO emissions, together with the quantification of recycled NO destruction, is discussed. This investigation finds that 85 % to

95 % of the recycled NO is destroyed at a range of burner configurations using OF 27 and OF 30 at 170 kW_{th}. In addition to this, NO formation and carbon burnout are found to be significantly affected with changing burner configurations. Further to this, OF 30 flames appear to be more sensitive to burner configuration than OF 27 flames with regards to both NO formation and destruction, possibly due to the decreased density of the OF 30 oxidant. Radial profiles of two burner configurations at OF 27 and OF 30, as well as an axial profile of two burner configurations at OF 30, are analysed. The profiles appear to show that burner staging aids in controlling the products of NO reburning, hence maximising the destruction of recycled NO.

INTRODUCTION

Oxy-fuel combustion is one of the most prominent carbon capture and storage (CCS) techniques, with a plethora of research being undertaken since the 1990s to better understand how to optimise this process. Subsequently, the technology has gained confidence and maturity [1] especially compared with much earlier studies [2-3]. Coal is the fuel of choice for many developing nations due to its relatively low cost and wide availability; therefore, in order to achieve worldwide CO_2 reduction targets, a concentration on achieving economical CCS techniques, for coal specifically, is key. Oxy-coal combustion involves using an O_2/CO_2 mixture as the combustion oxidant instead of air (an O_2/N_2 mixture). This has the effect of producing a flue gas with a much higher CO_2 concentration than combustion in air; therefore, greatly simplifying the purification/capture processes needed to ready the CO_2 stream for transport. However, due to the vast impurities present in coal and the lack of nitrogen's dilution effect, the concentration of pollutants and impurities in the flue gas are substantial. Further to this, it has been observed that the conversion of fuel-N to NO is markedly greater in an oxy-fuel flame, compared to an air flame [4], due to the increased oxygen concentration (25-35%) required in order to match the adiabatic flame temperature of an air flame [4-6].

For an oxy-fuel plant to achieve a target of near zero-emission, it would be necessary for selective catalytic reduction (SCR) [7] or sour compression [8] to be installed in order to tackle NO_x emissions. SCR is associated with costly catalysts that are subject to regular fouling, while sour compression could have a negative impact on the process economics due to the high pressures required; therefore, it is imperative to minimise NO formation and maximise destruction of recycled NO in order to minimise costs associated with these technologies.

Therefore, it is imperative to investigate the performance of low-NO_x burners during oxy-coal combustion, with particular emphasis on the impact of burner staging on the reburning of recycled NO.

LITERATURE REVIEW

During coal combustion, NO can be formed via three routes: thermal NO, prompt NO or fuel NO. Thermal NO is formed from the oxidation of elemental nitrogen present in the oxidant at high temperatures, becoming dominant above 1800 K [9]. Prompt NO is formed from the reaction of hydrocarbon radicals with elemental nitrogen early in the flame [10]. The greatest contributor of NO during coal combustion, however, is fuel NO. Nitrogen in the fuel is partitioned into either char or volatile-N; the former is either oxidised or left unburned, while volatile-N can form either NO or N2 depending on the local O2 concentration. During oxy-coal combustion, the flue gas is recirculated back into the flame in order to achieve the desired CO_2 mixture and a further phenomenon occurs, where a considerable portion of the recycled NO reacts with fuel fragments to produce N_2 [11]. Of this NO reduction, 50-80% is due to volatile-C reducing NO:

$$CH_i + NO \rightarrow HCN + products \qquad (1)$$

NO reduction on volatile-N accounts for 10-50%:

$$NH_i + NO \rightarrow N_2 + products \qquad (2)$$

The remaining reduction, >10%, is a complex series of reactions involving the reaction of NO with char in the presence of CO:

$$CO + C_{(O)} \rightarrow CO_2 + C_{(f)} \qquad (3)$$

$$NO + C_{(f)} \rightarrow C_{(O)} + \frac{1}{2}N_2 \qquad (4)$$

Where $C_{(O)}$ represents oxygen chemisorbed to char and $C_{(f)}$ represents an activated carbon site on the char [12].

These reburn reactions have been shown to lead to a 70-75% decrease in NO emissions compared to air firing [13]; while, at high temperatures, this study also claims that the Zeldovich mechanism can be reversed to further reduce NO. Various conditions must be reached for this process to be dominant, including very low air ingress, temperature higher than 1800 °C and decrease in temperature axially along the flame that is proportional to the NO concentration [14].

Prominent experimental studies [13, 15-17] provide confidence and understanding of the processes involved in low-NO_x oxy-fuel combustion, yet the majority of progress has been achieved either without staging or with in-furnace staging, as opposed to using burner staging which is widely utilised for air combustion. In-furnace staging involves creating a reducing (fuel-rich) zone initially around the burner and then introducing over-fire air in an oxidising zone to complete combustion. This concept has been studied for use in oxy-coal combustion to show that the fuel-rich zones cause greater NO reduction in oxy-combustion than in air and the NO concentration in the flue gas shows less sensitivity to the reducing zone stoichiometry than air [18]; further to this, it is believed that staged combustion in an O_2/CO_2 environment would lead to a significant reduction in NO_x emissions [19]. However within a commercial plant, NO

would be present in the over-fire stream of a commercial plant, and the utilisation of this form of staging could lead to a decreased rate of NO reduction [7]. Further to this, the primary zone created during in-furnace staging is highly reducing and the use of this technology under oxy-fuel conditions is likely to exacerbate any fireside corrosion issues in this portion of the furnace [7]. Further issues are identified in Ma, et al., (2017) [20]. Staging, when applied across the burner in low-NO_x burner technology, is known as burner staging and, due to recirculating flow patterns present in these flames, it is likely that the reburn rate of NO in this burnout oxidant will be higher than that of an over-fire stream.

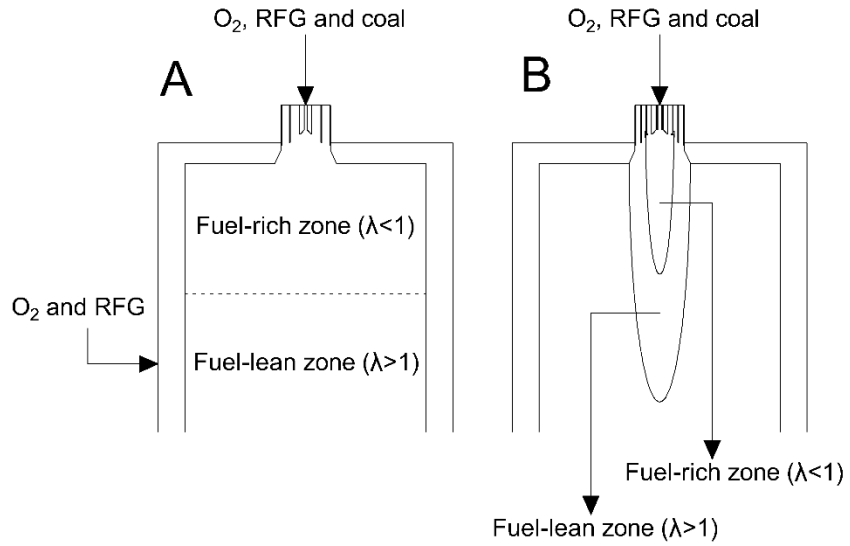

Figure 1. Diagrams of (a) in-furnace staging and (b) burner staging for oxy-coal combustion (adapted from Normann, et al., 2009 [21])

However, staging an oxy-fuel flame can present technical challenges; the structure is inherently different to that of an air fired one and in order to match the coal feed rate to an equivalent air fired plant, the velocity of the oxidant through the primary register must be matched [22]. Due to the greater density of the O_2/CO_2 mixture in comparison to air, the primary mass flow rate is higher; this leads to a lower secondary mass flow rate, as well as a

lower velocity of the secondary oxidant [23]. This can lead to complications regarding flame stability, often to which the required corrections compromise NO reduction. Liu, et al., [5] investigated maximising NO reduction without significantly affecting the flow dynamics by staging the input of recycled NO; this study finds that introducing the recycled NO into the primary or secondary leads to large NO reductions, but when NO is recycled into the tertiary stream, the reduction is greatly reduced. Unfortunately, staging NO introduction into the burner may not be feasible in a full-scale plant without significant cost. Alternatively, Chui, et al., [24] studied the effect of swirl burner configuration on NO reduction mechanisms; they found that increasing the swirl of the secondary stream increased residence time of fuel-N in the primary zone to promote N_2 formation pathways. Further progress led to the test of a new burner, achieving a further 70% reduction [25]. However, the recommendations from these studies have been described as individual to the tested burners and lacking transferrable conclusions that would aid further oxy-fuel burner research [7]. Conversely, valuable research has been carried out on the retrofit of air-fired burners for oxy-coal conditions, focussing on flame stabilisation by means of oxidant delivery [26] and swirl variation [27] encouraging a decrease in primary velocity compared to air conditions and a strong swirl respectively. Further to this, detailed emissions analysis was performed at 21 vol% and 25 vol% O2 and a fixed swirl highlighting trends between increasing O2 utilisation and decreased NO formation [28]; while, varied swirls were investigated in terms of emission measurements at the flue [29] and in-flame [30]. These studies confirm the significant impact of increasing swirl on a reduction in NO formation but there is little discussion of any impact on the destruction rates of recycled NO.

OBJECTIVE

This work aims at evaluating the use of low-NO_x burner technology in oxy-coal combustion with recirculated flue gas; while investigating the effect of burner settings of a popular

industrial low-NO_x burner on the minimisation of NO formation and destruction of recycled NO for low-NO_x operation of a pilot scale pulverised fuel (PF) combustion test facility (CTF). By means of the in-flame species measurements, emissions monitoring and imaging, this work aims to give insights into the structure of the flame produced as well as conditions within the furnace and the flue gas. This will aid in predictability for operators, in addition to providing greater understanding on the effect of controlled stoichiometric changes in the near-burner region on the NO destruction processes and providing an abundance of experimental trends to aid modellers.

EXPERIMENTAL SETUP

A large pilot scale 200 kW_{th} combustion test facility (CTF) (Figure 2) at the UK carbon capture and storage research centre's pilot-scale advanced CO_2-capture technology centre (UKCCSRC - PACT) has been utilised for the experimental data collection. The furnace of the 250 kW_{th} CTF measures approximately 4 m in height with an internal diameter of 0.9 m and contains a total of eight modular sections, each 0.45 m high and lined with 100 mm thick light weight alumina silicate refractory (Figure 3). A high density 96% alumina (thermally rated to 1850 °C) is used to cast the quarl section of the burner and the section connected to the quarl. The burner is a scaled down version of a Doosan Babcock Mk III low-NO_x burner; this consists of a primary annulus through which the coal is fed with a portion of the oxidant and the swirling secondary and tertiary annuli through which the remaining oxidant is delivered (Figure 4). A sliding partitioning damper controls the split between the secondary and tertiary oxidants; enabling a change in the stoichiometry in the near burner region and the overall swirl of the flame due to the larger swirl angle of the secondary register. The swirling primary oxidant carrying coal particles engages with the coal collectors for later mixing with swirling secondary and tertiary oxidant registers.

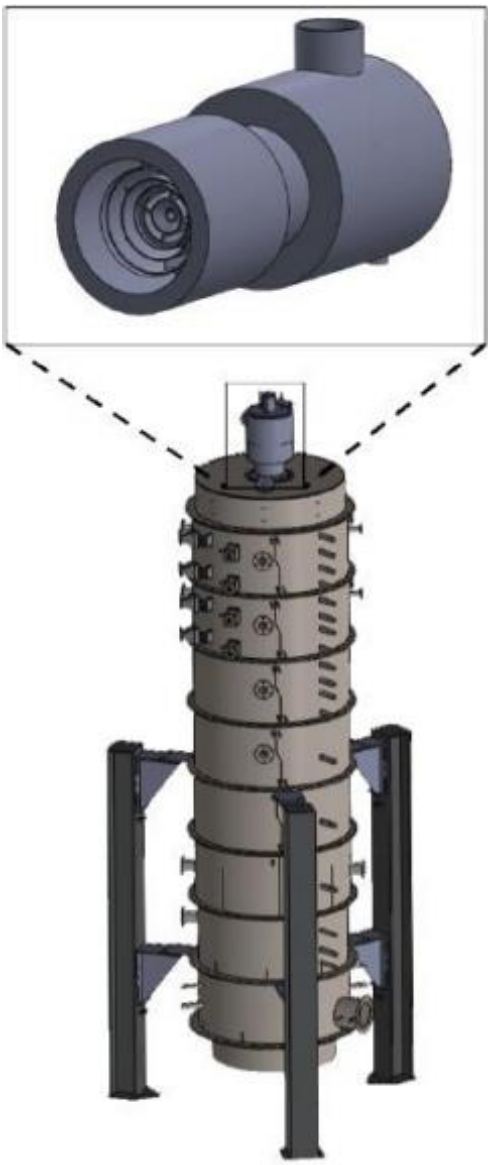

Figure 2. Layout of UKCCSRC-PACT oxy fuel combustion testing facility (250 kW_{th}) [31]

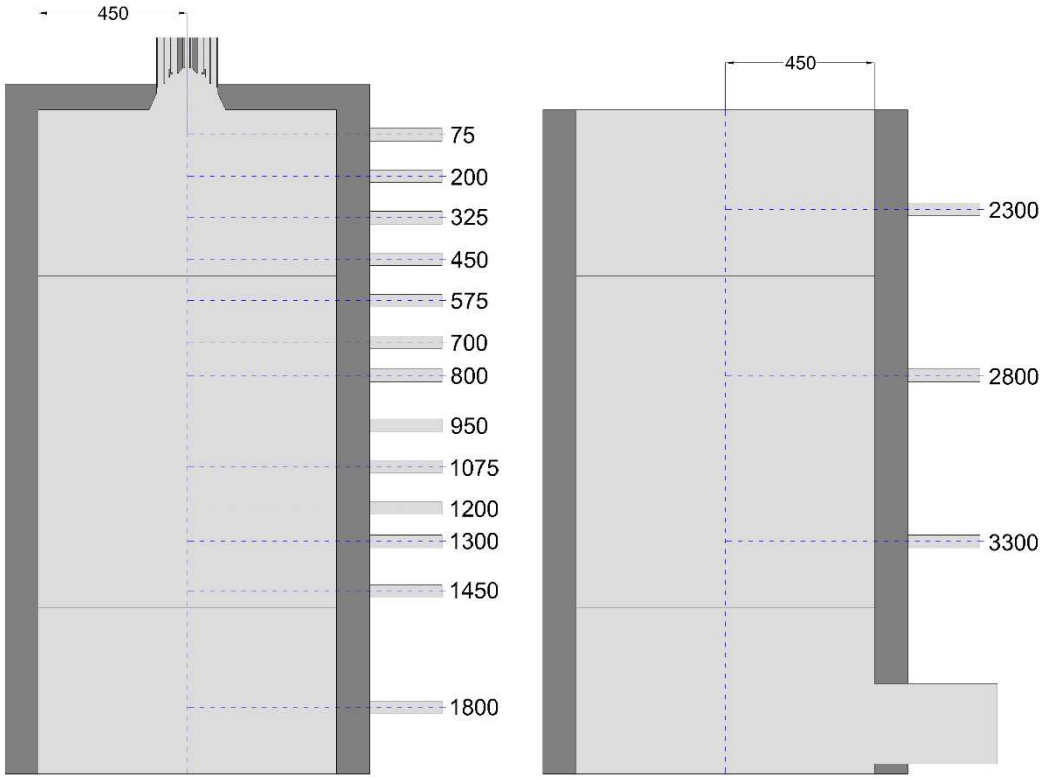

Figure 3. Furnace geometry and position of measurement ports

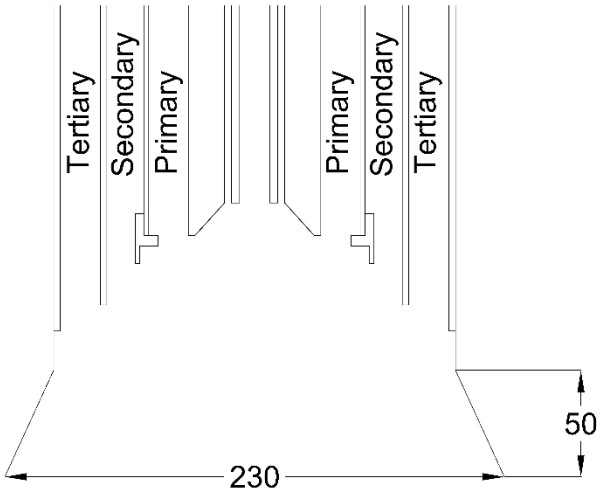

Figure 4. Burner dimensions (Adapted from Clements, et al., 2015) [32]

The oxidant is supplied from dedicated cryogenic storage tanks of O_2 and CO_2 through a dedicated primary compressor to a mass flow controlled manifold before entering to the primary, secondary and tertiary air registers. The desired O_2/CO_2 mass ratios in the respective

oxidant streams are also controlled in a separate dedicated oxy-manifold. The temperature of all the oxidant streams can be maintained using bespoke electrical heaters. The operating conditions for the baseline 200 kWth and the core 170 kWth tests can be found in Table 1. A separate 99.5% NO in N_2 injection manifold, with automatic shut-off safety valves, is used to inject NO into the O_2/CO_2 blend in order to simulate dry recycled flue gas. An induced draft fan (IDF) draws out the combustion products (fly ash and flue gas) from the bottom of the CTF; this then passes through a cyclone separator and a candle filtration unit (for fine particulate removal). The fly ash was collected and analysed after each test; this analysis involved heating to remove contaminants and moisture, weight measurements before and after the removal of moisture, heating in a muffle furnace to remove unburned carbon and then a final weighing. These values were then used to determine the quantity of unburned carbon in the sample under ISO:1171-2010.

		Primary Stream	Combined Secondary/Tertiary Stream
Air (200 kWth)	Air (kg/hr)	56	235
	Temperature (°C)	20	260
	Coal Feed Rate (kg/hr)	24.35	
OF 28 (200 kWth)	O_2 (kg/hr)	9	56
	CO_2 (kg/hr)	52	182
	Temperature (°C)	20	260
	Coal Feed Rate (kg/hr)	24.35	
OF 27 (170 kWth)	O_2 (kg/hr)	8	44
	CO_2 (kg/hr)	42	152
	Temperature (°C)	20	260
	Coal Feed Rate (kg/hr)	20.7	
OF 30 (170 kWth)	O_2 (kg/hr)	7	44
	CO_2 (kg/hr)	37	126
	Temperature (°C)	20	260

	Coal Feed Rate (kg/hr)	20.7

Table 1. Operating conditions

Natural gas is primarily used to heat up the CTF for roughly 2-2.5 hours before switching to pulverised coal combustion. The Cerrejón coal analysis tested as part of this study, sourced from Colombia, is given in Table 2. The conventional air-fired coal combustion takes approximately 1 hour to stabilise before the measurements can be recorded. The switchover from air to oxy-fuel is then initiated; this takes another hour to stabilise before measurements can be taken within the scope of the test. Each test is completed by swapping back to air-fired combustion from oxy-fuel combustion in order to check the coal feeding and sampling stability.

Ultimate Analysis (%)					Proximate Analysis (%)				Calorific Value (MJ/kg)
C	H	N	O	S	Moisture	Volatile Matter	Fixed Carbon	Ash	
74.50	5.04	1.58	18.50	0.38	5.12	36.90	56.06	1.92	29.57

Table 2. Cerrejón Coal analysis (as received basis)

During the tests, a variety of levels of NO were injected and mixed into different streams to simulate the recycled NO for both air and oxy-fuel cases. The concentration of the simulated NO injected was in the range of 122-1500 ppm, chosen from a review of available literature, and the reported NO destruction rates were calculated using (5):

$$NO\ destruction\ \% = 100 \times \frac{NO_{baseline} + NO_{recycled} - NO_{measured}}{NO_{recycled}} \qquad (5)$$

Where $NO_{baseline}$ are measurements taken without any recycled NO, $NO_{recycled}$ is the concentration of NO in the oxidant and $NO_{measured}$ are measurements taken when the NO concentration in the oxidant is equal to the value $NO_{recycled}$.

There are numerous ports along the combustor which could be used for the measurement of process temperature, flame shape recording and inflame emissions. Process thermocouples,

along with continuous emission monitoring equipment (i.e. NO_x, CO_2, CO, O_2, SO_2, and THC), are utilised for data gathering purposes for specific test runs. The data collected during the test gets logged every 5 seconds through supervisory control and data acquisition system connected to human machine interface (HMI). In-flame and flue gas samples are continuously drawn through a water jacketed probe via a Drechsel bottle (to remove dust and moisture) is connected to a temperature controlled heated ceramic gas filter. The pre-heated filtered gas sample is subjected to the temperature maintained fine filter element for further fine particle removal before dividing the sample into NO, NO_2 and to a cooler dryer splitting point feeding to the individual CO_2/O_2, CO and SO_2 analysers. To account for any drift in the instrument related measurement, calibrations are periodically performed before and during each test. Examples of flue gas composition when the ratio of secondary to tertiary oxidant is 45:55 are shown in Table 3 with an error of one standard deviation.

	CO2 (vol%, dry)	NO (ppmv, dry)	O2 (vol%, dry)
Air (200 kWth)	15.53 ± 0.16	329.80 ± 7.81	3.25 ± 0.12
OF 28 (200 kWth)	94.26 ± 0.51	281.94 ± 27.00	4.17 ± 0.90
OF 27 (170 kWth)	94.91 ± 0.20	208.32 ± 7.32	3.50 ± 0.30
OF 30 (170 kWth)	94.38 ± 0.20	195.79 ± 9.53	3.76 ± 0.39

Table 3. Raw flue gas composition when ratio of secondary to tertiary oxidant flow is 45:55

During data analysis, all NO measurements collected from the flue are corrected to 6% O_2; whereas, all in-flame NO measurements are reported as collected accompanied by the local O_2 concentration. Instantaneous flame images were recorded using a water-cooled optical probe inserted into the upmost section of the furnace. This probe contains a wide-angle lens that focuses light onto a complementary metal oxide semiconductor (CMOS) sensor of an industrial camera. The CMOS sensor allows videos of the flame to be recorded on a nearby laptop computer. Further information can be found in Farias Moguel, et al., (2018) [33].

The swirling vane angles are fixed, therefore it is important to comprehend that as the sliding partitioning damper is changed from 0 to 65 mm, the flow of the tertiary stream increases and the flow of the secondary stream decreases. This has the combined impact of decreasing the overall swirl of the flame and decreasing the amount the amount of O2 entering the near burner/fuel rich region. Hence, at a higher swirl, there is intensified mixing of oxidant (mainly primary and secondary), purported to result in higher NO due to greater oxidation of fuel-N. The impact of varying the proportion of burnout oxidant flowing through the secondary register on the individual stream velocities is shown in Table 4.

Velocity (m/s)										
170 kWth OF 27	200 kWth									
Primary	Air			OF 28						
	Primary	Secondary	Tertiary	Primary	Secondary	Tertiary				
2.88	4.98	18.22	0.00	3.54	13.15	0.00	100	Burnout Oxidant Passing Through the Secondary Register (%)		
		15.48	1.43		-	-	85			
		-	-		-	-	72			
		-	-		9.21	2.07	70			
		-	-		-	-	63			
		8.74	4.97		6.31	3.59	48			
		8.20	5.25		5.92	3.79	45			
		5.46	6.68		3.95	4.83	30			
		0.00	9.55		0.00	6.90	0			

		OF 30		
Secondary	Tertiary	Primary	Secondary	Tertiary
-	-		-	-
-	-		-	-
7.72	1.57		-	-
-	-		-	-
6.75	2.08	2.54	5.95	1.83
-	-		-	-
4.82	3.09		4.25	2.73
-	-		-	-
0.00	5.62		-	-

Table 4. Theoretical individual stream velocities for tested burner configurations

COMMISSIONING

Initially, baseline coal tests were completed at 200 kWth (Figure 5) to understand the influence of varying the proportion of overall air supplied to the primary register on the NO reduction and unburned carbon at burner configurations. An optimal primary to total oxidiser volume ratio was to be identified from these tests, which would be kept constant for all further oxy-coal investigations as recommended in literature [26, 34]. The air-coal combustion tests were performed by varying the primary air flow rate (between 16% and 22% of the total air flow) over a range of partitioning slide damper positions, in order to vary air flow rate through the secondary and tertiary registers and, hence, overall flame structure. It was observed that the flame routes were most stable and distinct when 20% of the overall air flowed through the primary register. This condition also provided slightly lower NO emissions as well as reduced unburned carbon. The overall trend shows that a secondary oxidant proportion of between 0.36 – 0.39 is optimal to achieve an adequate combustion efficiency and 310 - 320 ppm NO. The unburned carbon in this region, as shown in Figure 5,

is between 13 - 14 %. Study of the secondary/tertiary stream partitioning for the OF 28 case was undertaken in order to ascertain the effect on unburned carbon and NO emissions; this is plotted in Figure 5. OF 28 case tests were only performed with the primary containing 20% of the overall flow due to the flame stability consensus formed from air combustion tests.

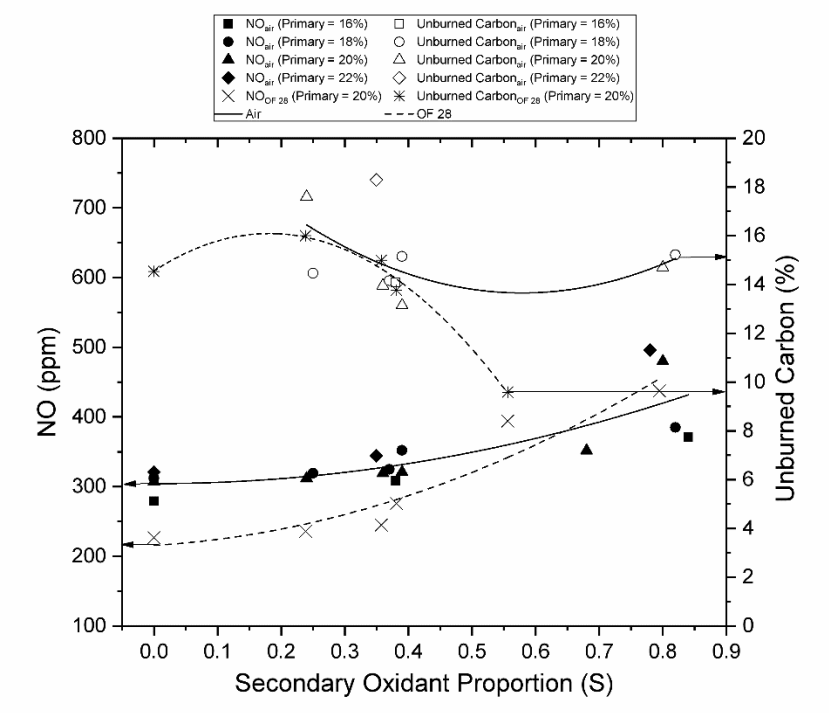

Figure 5. The effect of varying the secondary oxidant proportion on NO emissions and unburned carbon for the air and OF 28 cases (as well as varying the portion of overall oxidant flowing through the primary register for the air case)

It can be concluded from both air and OF 28 cases that by varying the split of oxidant (air or OF 28) flow in order to increase the tertiary flow produces relatively reduced swirls, which favours the control of NO through supporting the production of volatile-N over char-N. It is pertinent to mention that due to the lack of dilution by N_2, NO emissions reported in ppm are expected to be greater for the OF 28 case in comparison to air combustion [35, 36]; however, due to the staging of the flame, and possibly greater CO and hydrocarbon concentrations in the fuel-rich zone, higher reduction of NO is observed [4] leading to reduced overall NO

emissions (225-275 ppm). Figure 6 shows the comparative plots for NO_x reported in mg/MJ. The reduced secondary oxidant proportion also has the impact of reducing the availability of oxygen to the fuel-rich zone, from the decrease in the secondary flow rate, within the flame enabling lower NO formation. The near lack of N_2 in the oxidant would, also, cause far less formation of thermal NO. In addition, the reduced O_2 availability in the fuel-rich zone leads to an increased CO concentration; this would enhance reduction of generated NO on surface char [37]. The combination of these phenomena results in an S of 1.45 to 1.55 producing the optimum conditions with regards to NO production and unburned carbon. As shown in Figure 6, OF 28 only produces just over 50% of NO that the air case produces at a S of 1.50, which is comparable to the levels reported [4] for a OF 30 case.

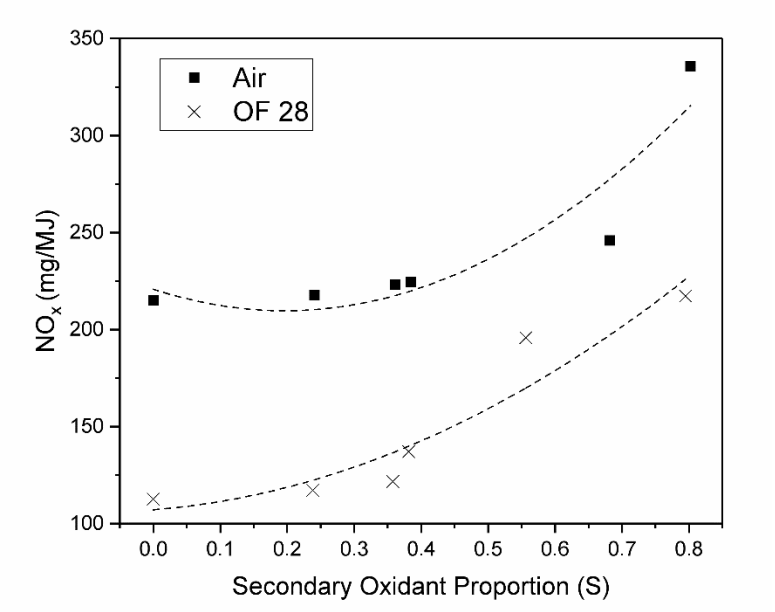

Figure 6. The effect of varying secondary oxidant proportion on emissions of NO_x, reported as NO_2, for air and OF 28 cases through altering the secondary/tertiary split

The data obtained from the OF 28 cases provided far greater spread than was expected, as can be seen from the large standard deviations in Table 3. Therefore, the burner was turned down by 15% (i.e. thermal capacity was reduced to 170 kW_{th}) in order to reach steady state more promptly during the test day allowing for greater and more precise measurements. For this

new thermal capacity, 27% oxy-fuel was used instead of 28% oxy-fuel for two reasons: 1. In order to provide greater disparity between the high (OF 30) and the low (OF 27 and 28) oxygen results so there is more clarity in any diverging trends; and 2. The concentration of oxygen in the primary stream was increased to 21% from 18.5%, in order to reduce any flame stability issues that may be aggravating the spread of the data, and so 27% oxy-fuel was used in order to discourage direct emissions comparisons between the 200 and 170 kWth data.

RESULTS

Recycling NO in OF 27 and OF 30 at 170 kW_{th}

Maintaining the primary as 20% of the total flow, as recommended from Figure 5, the secondary oxidant proportion (S) was varied for OF 27 and a variety of NO injection rates were utilised. The NO emissions in the flue were recorded, along with the unburned carbon in the ash. In addition to this, the NO emissions from two OF 30 cases were also recorded. The secondary oxidant proportions for the OF 30 case were chosen by using the secondary/tertiary split that resulted in both acceptable unburned carbon as well as low NO emissions from the OF 27 case. As can be seen from Figure 7, the burnout for the OF 27 case was greatly affected by the burner configuration, with the unburned carbon dropping greatly as secondary oxidant proportion was increased; this is due to the increased availability of oxygen to and greater mixing into the fuel-rich zone at higher swirls.

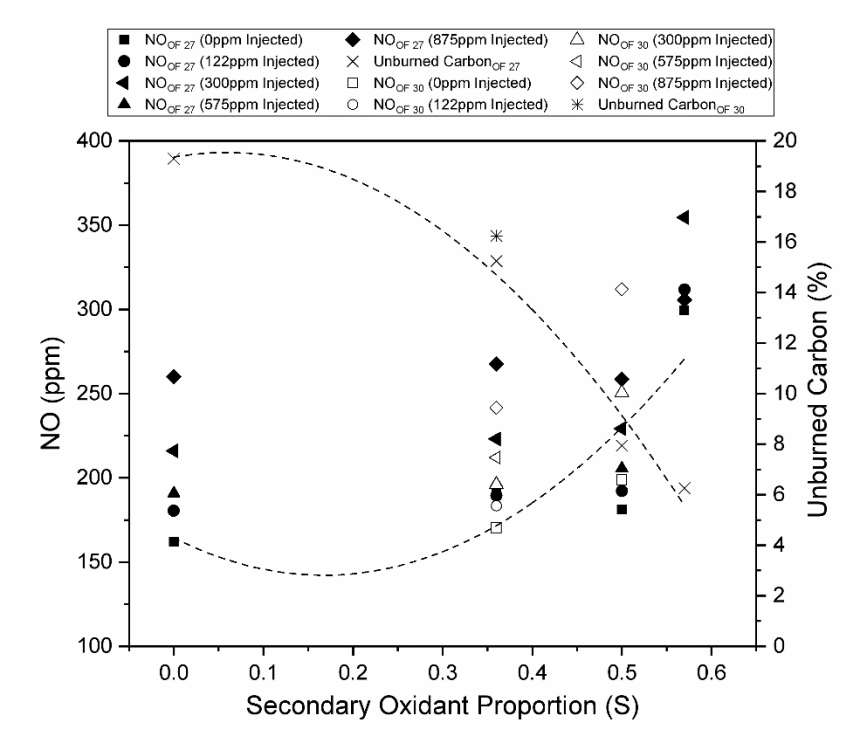

Figure 7. The effect of varying the secondary oxidant proportion and recycled NO on NO emissions and unburned carbon for the OF 27 and OF 30 cases

The optimal S was found to be 0.50 for OF 27; whereas, the same configuration when used for the OF 30 case showed dramatically increased NO emissions compared to when an S of 0.36 was used. The greater NO formation is attributable to the greater flow of oxidant through the secondary register, increasing swirl and the mixing of oxygen with fuel in the near-burner zone and creating a less fuel-rich zone. When compared to the equivalent OF 27 cases, the same phenomenon is not witnessed until a higher secondary oxidant proportion (S : 0.57); this is believed to be due to the increased oxygen concentration and lower gas volume at OF 30 causing more efficient oxidation of the fuel-N. The NO emissions from the OF 30 case at an S of 0.36 are lower than at the equivalent burner configuration for OF 27; this could be due to the decreased density of the oxidant creating a weaker swirl, resulting in poorer mixing of oxygen into the fuel-rich zone and fewer NO formation reactions. Alternatively, this difference could result from the higher temperature OF 30 flame

influencing the char/volatile split in favour of volatiles [38, 39], as well as marginally reducing char-N to NO conversion rates [40], as seen in Figure 8 with temperature readings from four thermocouples in the upper portion of the furnace, or from the elevated oxygen concentration [41].

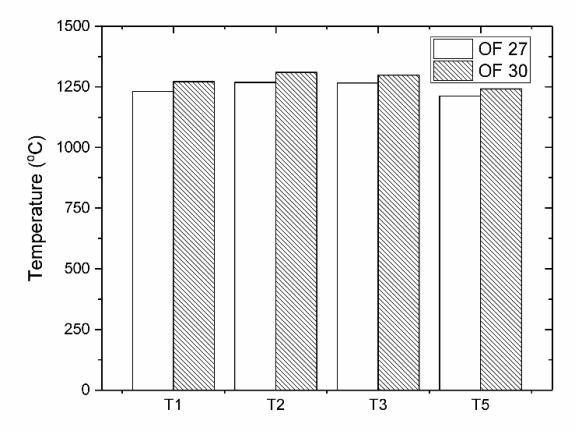

Figure 8. A comparison temperature readings from the upper portion of the furnace for OF 27 and OF 30 cases at S of 0.36

Instantaneous images of the flames investigated in Figure 7 is shown in Figure 9. The change in flame shape witnessed is pronounced and can be used to further explain the relationships witnessed in Figure 7. As the tertiary flow decreases and the secondary flow increases reciprocally, the swirl increases due to the greater swirl angle of secondary register; this leads to a shorter and wider flame. These factors will increase the mixing of oxygen into the fuel-rich zone, hence significantly increasing carbon burnout and NO formation.

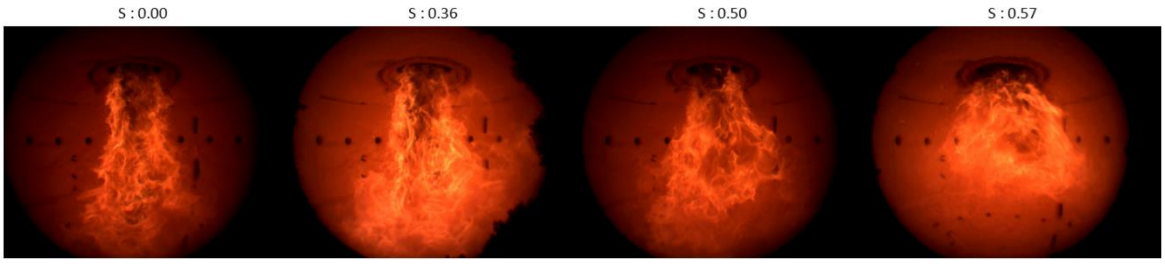

Figure 9. Instantaneous flame images at OF 27 170 kW_{th}

The rate of destruction of recycled NO are shown for each case in Figure 10; these will indicate any variation to reburning processes caused by a change in burner configuration. The destruction rates are greater than 80% for every burner configuration at each oxy-fuel case. For the OF 27 cases, there is only a very slight sensitivity to burner configuration, with the extreme configurations, S of 0.00 and 0.57, being the only cases to vary significantly from 90% destruction; the latter of these approaches 100 % reduction at two of the recycling regimes, most likely due to the increased secondary flow promoting transfer of NO into the fuel-rich region. The increased presence of initial NO in the fuel-rich zone may also be contributing to the inhibition NO formation, which could slightly distort NO destruction rates, implying higher greater NO reburning. It is also prevalent to mention that for individual burner configurations, the NO destruction rate remains quite stable as the level of recycled NO is increased, implying that the limit to NO reduction is the attainment of an reduction/oxidation equilibrium comprising of the reduction of NO with volatile-C to produce volatile-N and the oxidation of this volatile-N to reproduce NO.

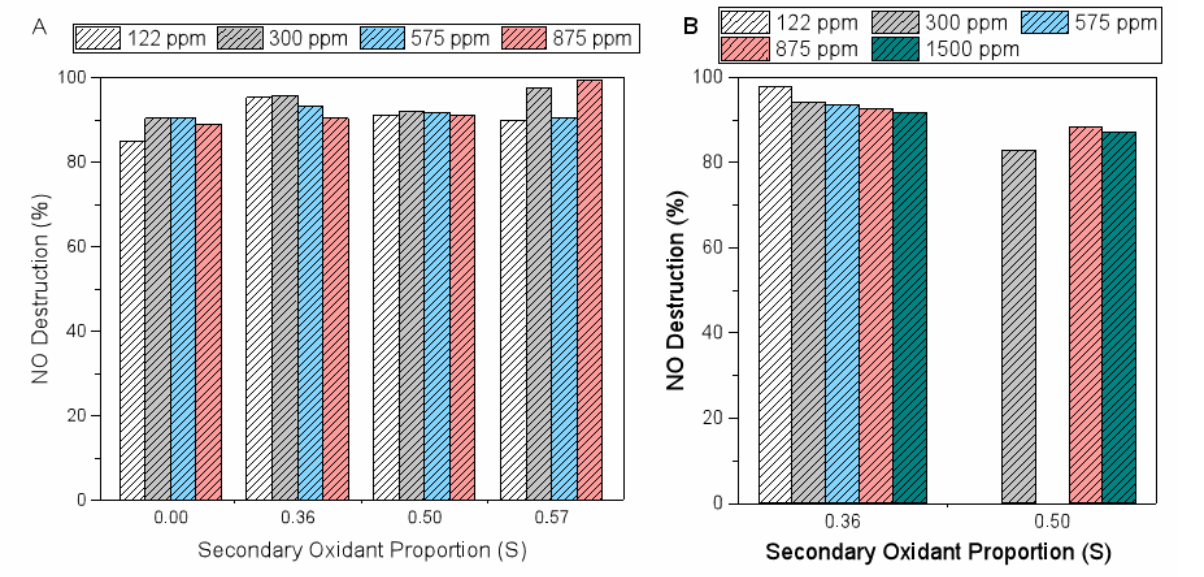

Figure 10. The effect of varying secondary oxidant proportion and recycling regime on the destruction of recycled NO for the OF 27 (A) and OF 30 cases (B)

The OF 30 case at an S of 0.36 not only leads to lower NO emissions but also slightly improved NO destruction over the equivalent OF 27 case. However, this improvement in NO destruction is not seen at the higher secondary oxidant proportion of 0.50, which, although not all NO recycling regimes could be tested, shows worse NO destruction rates compared to the OF 27 case. These trends are further highlighted in Figure 11, which displays the NO_x emissions reported in mg/MJ. The difference between NO_x emission rates at OF 27 and OF 30 using an S of 0.36 grows as a greater amount of NO is recycled into the burner; whereas at an S of 0.50, the NO_x emission rate is only slightly improved for the OF 30 case when there is no recycling, but this position greatly deteriorates as NO_x is recycled, due to the decreased density at OF 30 creating a weaker swirl compared to the same burner configuration at OF 27 and this weaker swirl perhaps compromising the residence time of recycled NO within the fuel-rich zone.

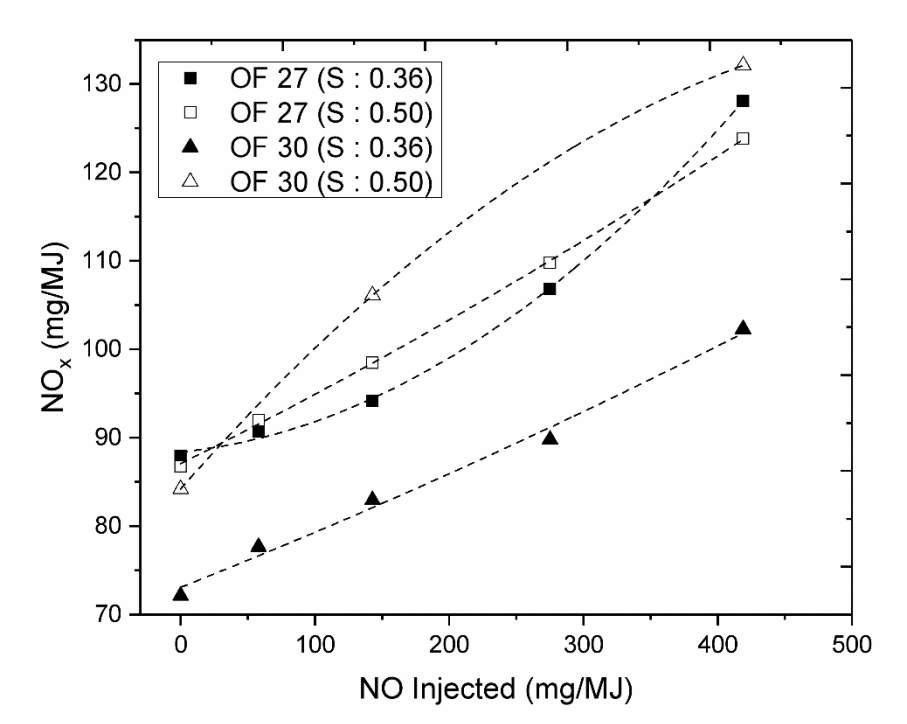

Figure 11. The effect of varying recycled NO on emissions of NO_x, reported as NO_2, for OF 27 and OF 30 cases at equivalent burner configurations

Figure 12 shows instantaneous flame images of the two OF 30 flames being investigated in this study. The smaller flue gas volume at OF 30 leads to less variation in the flame shape between the two burner configurations when compared to the equivalent cases at OF 27; this leads to a less wide S : 0.50 flame at OF 30, which could be an indication of a weaker swirl caused by the decrease in oxidant density.

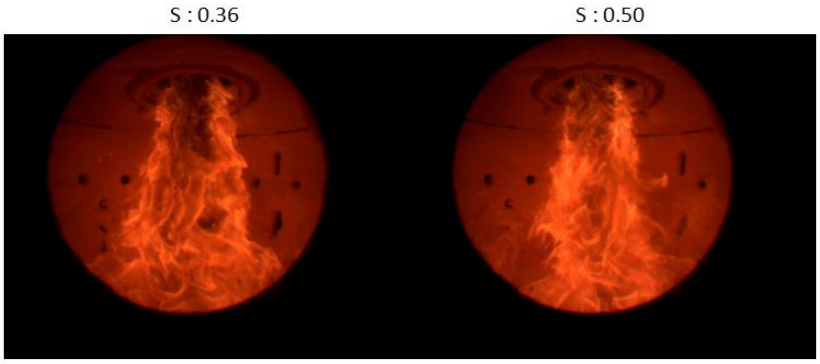

Figure 12. Instantaneous flame images at OF 30 170 kW_{th}

In-flame Analysis of NO Recycling in OF 27 and OF 30 at 170 kW_{th}

Figure 13 displays species measurements across a radial profile at 75 mm downwards from the burner for the OF 27 case with varying amounts of recycled NO. These radial profiles represent the impact of recycled NO on various constituents of the oxy-fuel flame. The most significant differences can be seen in the NO radial profiles. Without any recycled NO, an initial destructive zone can be observed between 0 and 25 mm that leads to roughly half of the NO being destroyed. When increasing amounts of NO are recycled, this decrease in NO becomes less and then disappears for the 1500 ppm case with a slight increase in NO. In actuality, the phenomenon displayed here is the destruction of a proportion of recycled NO; for the 1500 ppm NO case, there is an increase of roughly 600 ppm (in comparison to the 0 ppm NO case at 25 mm) and, therefore, about 60% of the recycled NO in that area has been destroyed. At 75 mm, the impact of the shear boundary can be witnessed as volatile-N is

rapidly oxidised by O_2 diffusing into the fuel-rich zone from the secondary stream. The increase in NO from 25 mm to 75 mm decreases as the quantity of recycled NO increases, implying there is less volatile-N present for the 1500 ppm case and possibly highlighting the importance of the advanced reburn reactions (involving NH_3 and HCN). Variation of the CO and O_2 radial profiles between recycling regimes shows little semblance of a consistent relationship between the variables; this implies that any effect on CO concentration through interaction with NO (in the presence of char) is surpassed by the slight impact of NO on combustion processes. The THC concentration, however, varies dramatically depending on the NO recycling scheme; for the 1500 ppm NO case, the THC in each region is far less than the baseline (0 ppm) case. This indicates that the recycled NO is playing a prominent role in the oxidation of hydrocarbon fragments; this confirms the work of Okazaki and Ando [5] [], that the reaction of NO with volatiles (both volatile carbon and nitrogen) has a far greater effect than reduction of NO on char.

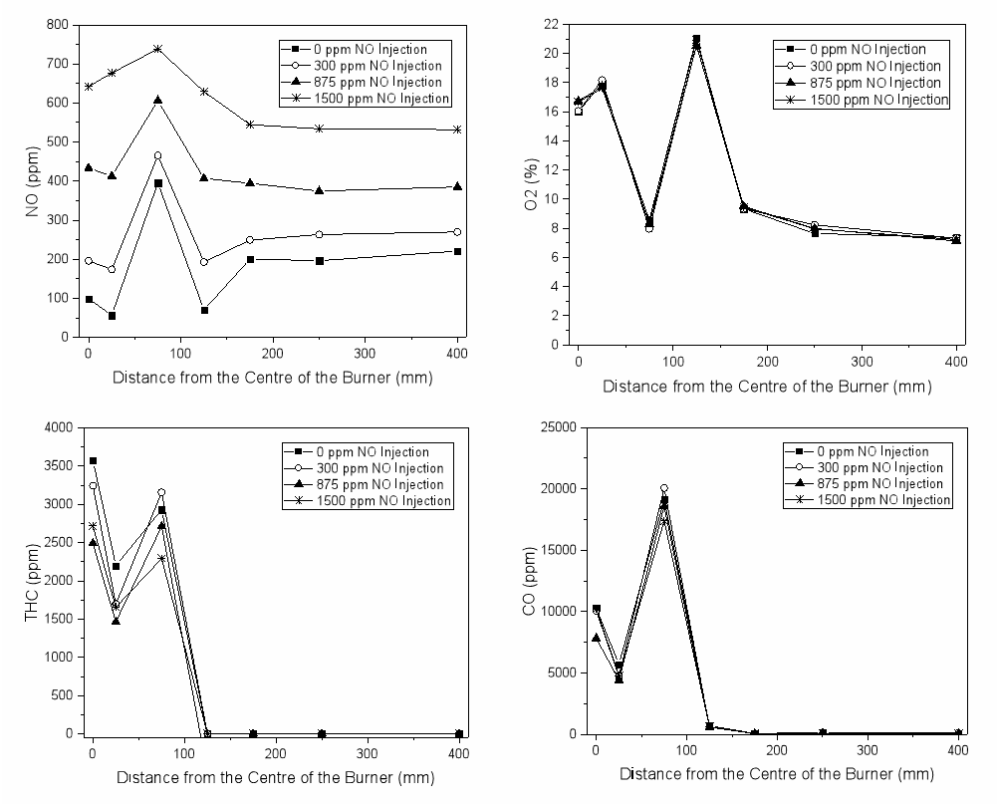

Figure 13. Radial profile mapping from the centreline of the burner of key flame constituents at 75 mm from the burner for the OF 27 case at S of 0.36

Figure 14 compares the radial profile of key gas constituents at 75 mm from the burner using two slightly varied burner configurations for the OF 27 case. A scenario without NO recycling and one utilising 300 ppm NO in all streams of the oxidant are presented. As can be observed, the NO measured for the case at S of 0.36 is lower than the NO measured for the case at S of 0.50 at each sampling site, except at 125 mm where there is a large degree of dilution, as can be observed from the high O_2 concentration at this point, from the incoming secondary oxidant. The combustion can be considered to be worse in the inner recirculation zone (IRZ) points (0 and 75 mm) for the case at the S of 0.50 due to the considerably greater THC and CO concentrations, however this implies that this region is more fuel rich. The impact on NO reburning can be indicated from the difference between values recorded with and without NO injection at each burner configuration. At 0 mm, the difference between NO values at each NO injection regime at S of 0.50 is less than at S of 0.36, indicating that NO

reburning is improved at this point, most likely because it is more fuel rich. The decreased tertiary oxidant flow rate at S of 0.50 leads to an external recirculation zone (ERZ) with a lower O_2 concentration, witnessed in Figure 14 from (175 mm to 400 mm). As the ERZ recirculates to the root of the flame, less O_2 is available to be transferred into the IRZ, leading to the lower O_2, higher THC and CO at 0 mm. Unlike at S of 0.36, the presence of injected NO at S of 0.50 leads to increased THC and CO, indicating a decreased combustion efficiency. Therefore, at OF 27, although a more fuel-rich zone is created and the NO reburning rate is slightly increased as a result, the increased NO formation is too great at S of 0.50.

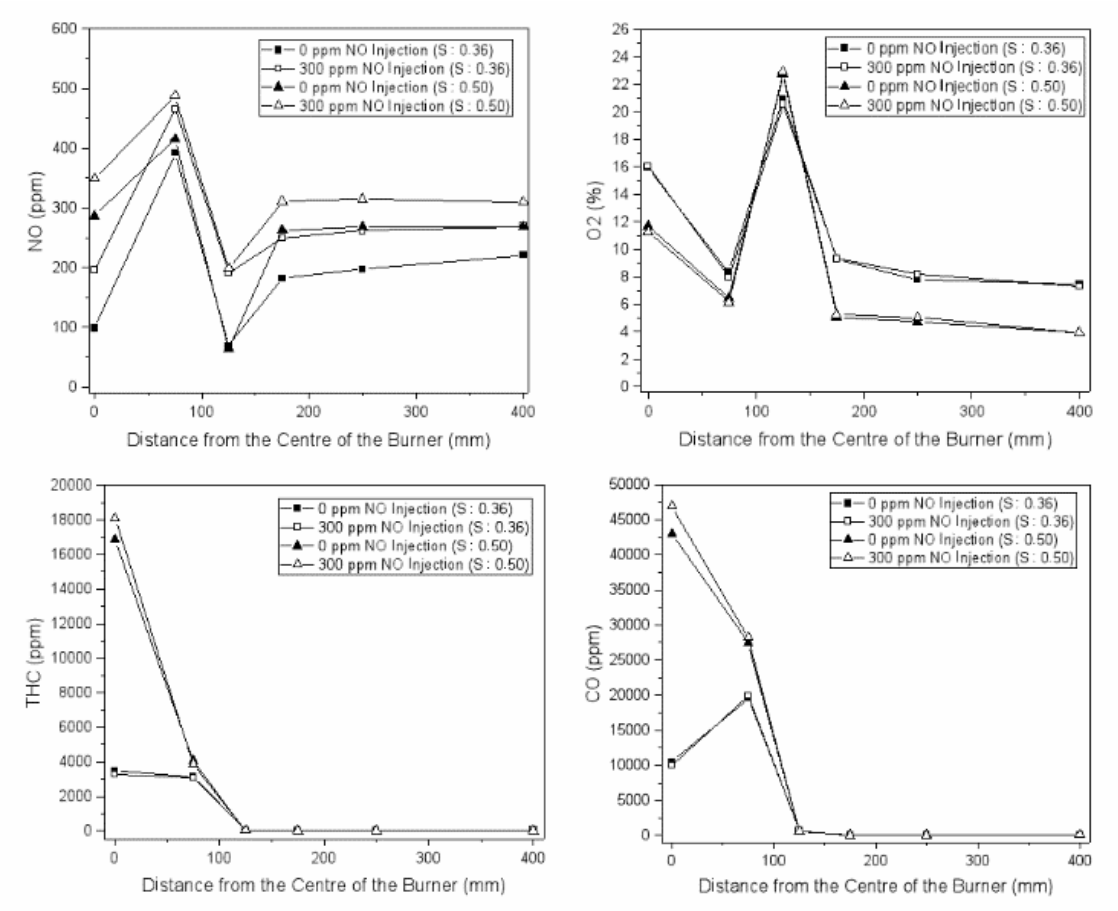

Figure 14. Radial profile mapping from the centreline of the burner of key flame constituents at 75 mm from the burner for the OF 27 case at S of 0.36 and S of 0.50

Figure 15 compares the radial profile of key gas constituents at 75 mm from the burner using two burner configurations for OF 30. As in Figure 14, a case without NO recycling and another utilising 300 ppm NO in all streams of the oxidant are analysed. As can be observed, the NO measured for the case at S of 0.36 is lower than the NO measured for the case at S of 0.50 at the area between 0 mm and 75 mm from the centreline of the burner. Further to this, when 300 ppm of NO is injected, the increase in NO, as well as THC and CO, concentration for the case at S of 0.50 is far greater than the case at S of 0.36, which is contrary to the equivalent cases at OF 27; these increases are considerably larger than at OF 27 and is most likely due to an anomalous deficiency of O_2 recorded at this point. The change in NO from the dilution point (125 mm) to the start of the ERZ (175 mm) is different for the two injection regimes; the larger increase for the 0 ppm case implies that a larger amount of volatile-N remains to be oxidised within the burnout oxidant and, therefore in the 300 ppm case, the recycled NO is subject to advanced reburning, reducing the volatile-N content. NO concentrations past the 175 mm mark are similar for each burner staging environment, suggesting that the impact of a decreased tertiary flow rate for the case at S of 0.50 has little impact on the ERZ at OF 30, as opposed to the case at OF 27. This phenomenon could be attributable the fact that the total mass flow rate of oxidant during OF 30 operation is considerably lower and, due to this, the flame is likely smaller; therefore, the flue gas recirculating in the ERZ has originated from a location in the furnace where the chemistry is more resolved than for the OF 27 case. The impact of this phenomena is that there is a decreased variation between burner staging environments at 0 mm, compared to OF 27, and, hence, burner staging characteristics can vary between oxy-fuel regimes.

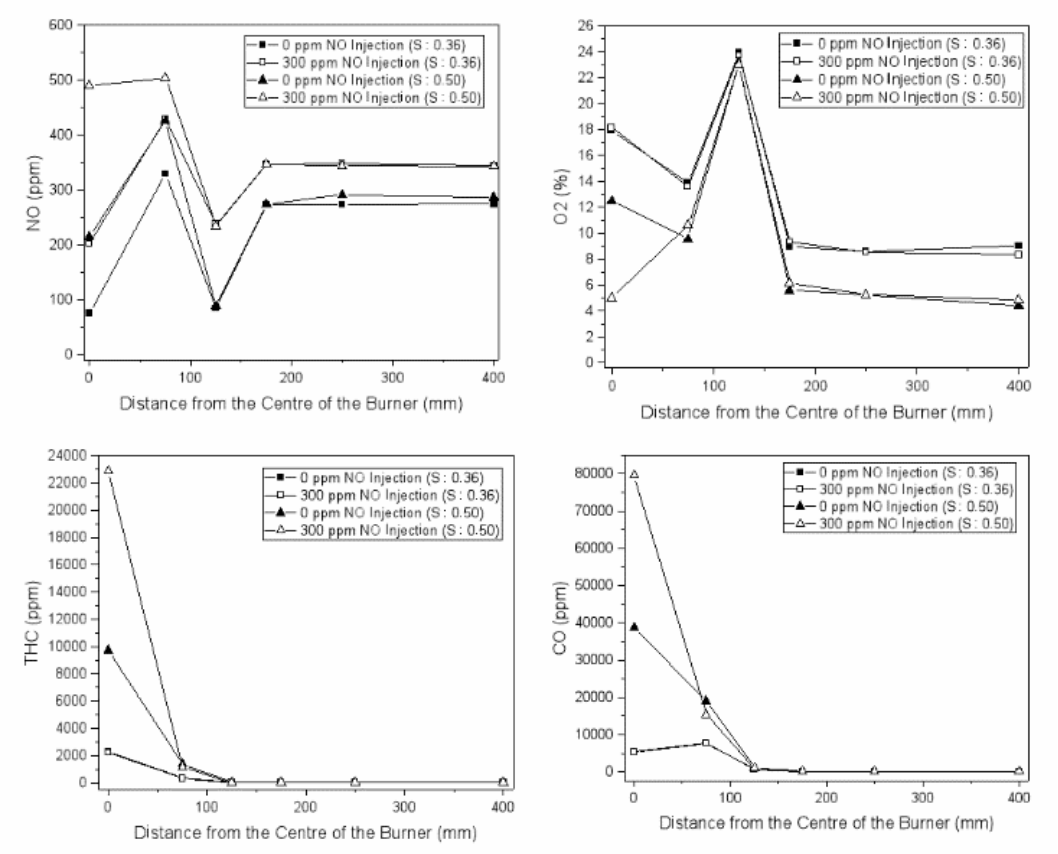

Figure 15. Radial profile mapping from the centreline of the burner of key flame constituents at 75 mm from the burner for the OF 30 case at S of 0.36 and S of 0.50

Figure 16 compares the profiles of key gas constituents axially down the centreline of the furnace between the cases at S of 0.36 and S of 0.50 for OF 30. Initially, as also seen in Figure 15, NO formation is increased for the case at S of 0.50 (compared to S of 0.36), however as the furnace is descended the NO concentration for the case at S of 0.36 increases past the values for the case at S of 0.50, indicating NO formation is delayed for the case at S of 0.36. This delay in NO formation seems to have little effect on the reburning capacity, as there is a high level of destruction witnessed here for both cases. The minimum NO, for both cases, is witnessed at 800 mm and is a culmination of the great drop in THC from the peak witnessed at 375 mm partly caused by the reburning of formed NO; during this period, the O_2 is depleted for both cases, which would facilitate this NO destruction. The return of

significant O_2 presence post-800 mm leads to a slight increase in the NO; this is possibly due to the oxidation of volatile-N that can be formed from reactions between NO and THC.

The axial profile can be considered to consist of three zones: the first involves the creation of the reducing species (THC, NO etc) (75-325 mm), the second involves the destruction of these species in an oxygen deficient environment (325-800 mm) and the third involves the oxidation of the remaining species (800 mm onwards). However, this simplification is complicated by the introduction of recycled NO, which is almost entirely destroyed within the first zone. It is likely that this phenomenon will produce a flame with an increased level of volatile-N, which would posit to explain why the NO increase within the oxidation zone is greater for the case with 300 ppm of NO being injected. This could also be due to the reduced destruction of NO entrained in the tertiary stream; however, the destruction of NO entrained in solely in the secondary and tertiary stream should remain significant [5]. It is, therefore, preferable to control this additional volatile-N using the fuel-rich zone to prevent conversion back to NO.

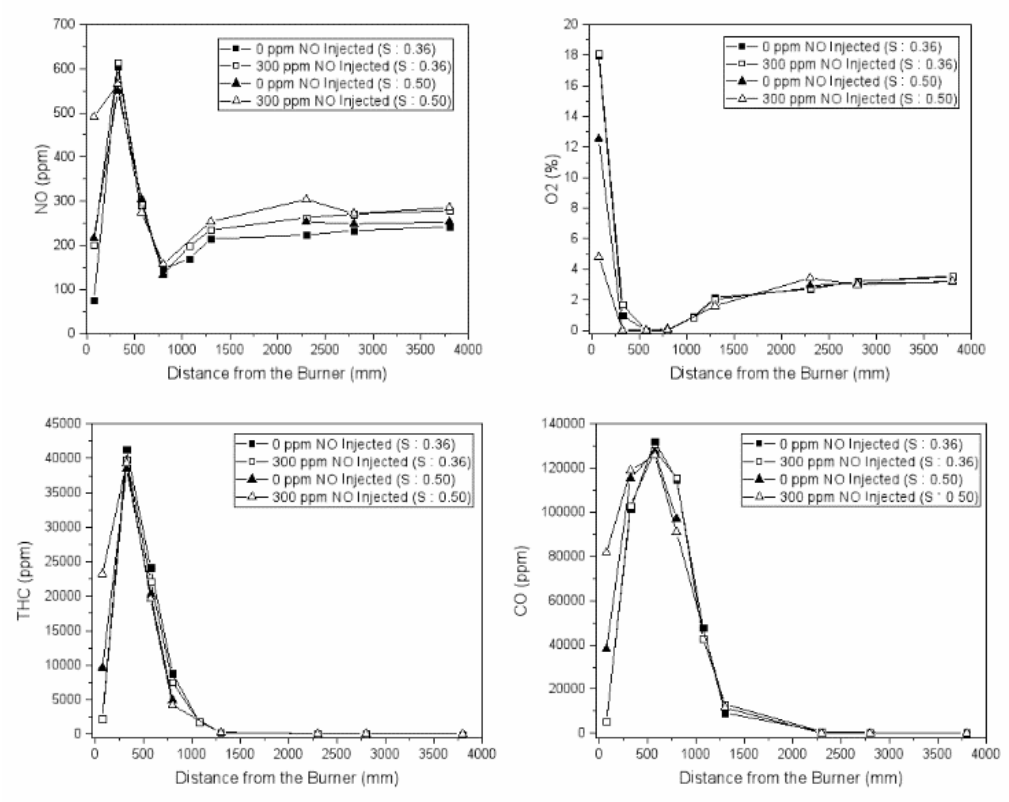

Figure 16. Axial profile mapping down the centreline of the burner of key flame constituents from the burner for the OF 30 case at S of 0.36 and S of 0.50

Figure 17 shows a diagram identifying the position of distinct zones within a furnace when using a single swirled flame, such as the one investigated in this study. However, a practical coal-fired boiler is likely to have many burners in series, each affecting the other aerodynamically and chemically. It is, therefore, important to explore theoretical divergences from the data in this study. One impact may include a discrete change in the chemical composition of the jet expansion zone (JEZ) due invasion of flue gas from opposing or parallel flames; this would in turn affect the chemical composition of the ERZ, which is crucially fed back to the root of the flame, invalidating the ERZ measurements in this study. Another key impact could be a disruption of the eddies within the ERZ, which could lead to change in how quickly heat and species are recirculated to the root. On the other hand, it is likely the IRZ and the actions at the shear surfaces within the flame would be minimally

affected by flames in series and, therefore, the impacts of burner configuration on NO reburning described are likely valid for a full-scale boiler.

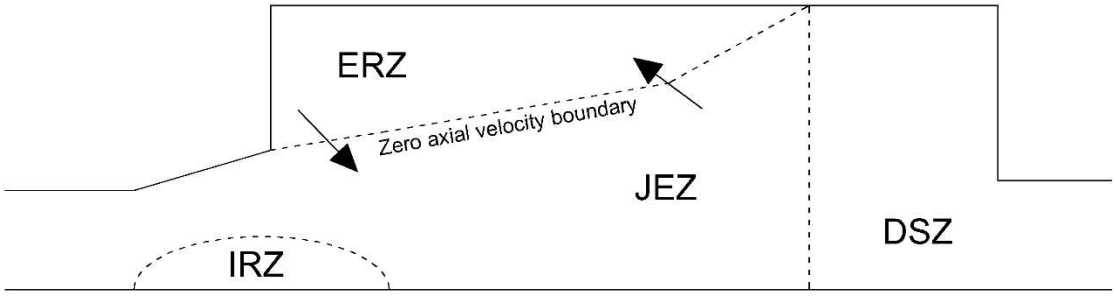

Figure 17. Distinct zones present in a furnace with one swirl burner (Adapted from Pedersen, et al., [42])

CONCLUSIONS

This investigation has studied the effect of various burner configurations on the NO_x emissions and destruction of recycled NO during oxy-coal combustion. These burner configurations have been achieved by altering the volumetric flow rate of the secondary and tertiary oxidant flows using a partitioning slide damper; it has been assumed that this would have the effect of altering the stoichiometry within the fuel rich region by increasing the swirl of the flame and promoting mixing of oxygen from the secondary stream into the fuel-rich region. It has been shown that recycled NO destruction rates are high and remain stable across a range of burner configurations for the OF 27 case; however for the OF 30 case, there is a noticeable decrease in NO destruction when the secondary oxidant proportion is increased. This was believed to be due to the decreased density of the OF 30 oxidant causing a weaker swirl and, therefore, compromising the residence time of the recycled NO within the fuel rich region compared to the OF 27 case. The NO formation rates and burnout of the fuel varies significantly across the tested burner configurations. For the OF 27 case, the NO_x emissions varied from 77 to 143 mg/MJ and the unburned carbon in ash decreased from

around 19% to 6% for S between 0.00 and 0.57. For the OF 30 case, the NO_x emissions were measured at 72 mg/MJ at an S of 0.36, but rose to 84 mg/MJ when the S was increased to 0.50. The increased NO formation was believed to be caused by the increased secondary stream providing more oxygen and promoting greater mixing with the fuel-rich zone.

Radial profiles of key gas constituents were taken 75 mm from the burner at a range of NO recycling regimes, two burner configurations and two oxy-fuel regimes, as well as axial profiles down the centreline of the furnace for two burner configurations at OF 30. It has been theorised that not only is burner staging preferable for controlling NO formation from combustion, but also acts to manage the products of NO reburning in order to prevent the reformation of NO. By studying two moderate burner staging environments, which differ slightly through the flow rates of the secondary and tertiary oxidant streams, we are able to describe how slight changes in the flame structure effect pollutant formation and combustion progress during oxy-coal combustion.

AUTHOR INFORMATION

Corresponding Author

*s.daood@sheffield.ac.uk (S. S. Daood)

Author Contributions

The manuscript was written through contributions of all authors. All authors have given approval to the final version of the manuscript.

Funding Sources

The Engineering and Physical Sciences Research Council EPSRC grants (UKCCSRC-C1-27, Experimental investigation and CFD modelling of oxy-coal combustion on PACT facility with real flue gas and vent gas recycling).

ACKNOWLEDGMENT

The authors would like to acknowledge the support from the Engineering and Physical Sciences Research Council EPSRC grants (UKCCSRC-C1- 27, Experimental investigation and CFD modelling of oxy-coal combustion on PACT facility with real flue gas and vent gas recycling). The experimental data was obtained by running experiments at the UKCCSRC PACT Facilities, funded by the Department for Business, Energy & Industrial Strategy (BEIS) and the Engineering and Physical Sciences Research Council (EPSRC). The authors are particularly grateful to Martin Murphy and Oscar Farias Moguel for their help operating the CTF.

ABBREVIATIONS

CCS	Carbon capture and storage
CMOS	Complementary metal oxide semiconductor
CTF	Combustion test facility
DSZ	Down-stream zone
ERZ	External recirculation zone
HMI	Human machine interface
IRZ	Inner recirculation zone
JEZ	Jet expansion zone
LNB	Low NOx burner
OF	Oxy-fuel
PF	Pulverised fuel

SCR Selective catalytic reduction

UKCCSRC – PACT UK carbon capture and storage research centre – pilot-scale advanced CO2-capture technology centre

REFERENCES

(1) Fujimori, T.; Yamada, T. Realization of oxyfuel combustion for near zero emission power generation. *Proc. Combust. Inst*. **2013**, *34* (2), 2111-2130. https://doi.org/10.1016/j.proci.2012.10.004.

(2) Kimura, N.; Omata, K.; Kiga, T.; Takano, S.; Shikisima, S. The characteristics of pulverized coal combustion in O2/CO2 mixture for CO2 recovery. *Energy Convers. Manage.* **1995**, *36* (6-9), 805-808. https://doi.org/10.1016/0196-8904(95)00126-X.

(3) Wang, C. S.; Berry, G. F.; Chang, K. C.; Wolsky, A. M. Combustion of pulverized coal using waster carbon dioxide and oxygen. *Combust. Flame*. **1988**, *72* (3), 301-310. https://doi.org/10.1016/0010-2180(88)90129-0

(4) Liu, H.; Zailani, R.; Gibbs, B. M. Comparisons of pulverised coal combustion in air and in mixtures of O2/CO2. *Fuel*. **2005**, *84* (7-8), 833-840. https://doi.org/10.1016/j.fuel.2004.11.018.

(5) Liu, H.; Zailani, R.; Gibbs, B. M. Pulverized coal combustion in air and in O2/CO2 mixtures with NOx recycle. Fuel. 2005, 84 (16), 2109-2115. https://doi.org/10.1016/j.fuel.2005.04.028.

(6) Croiset, E.; Thambimuthu, K.; Palmer, A. Coal combustion in O2/CO2 mixtures compared with air. *Can. J. Chem. Eng*. **2000**, *78* (2), 402-407. https://doi.org/10.1002/cjce.5450780217.

(7) Toftegaard, M. B.; Brix, J.; Jensen, P. A.; Glarborg, P.; Jensen, A. D. Oxy-fuel combustion of solid fuels. *Prog. Energy Combust. Sci*. **2010**, *36* (5), 581-625. https://doi.org/10.1016/j.pecs.2010.02.001.

(8) Murciano, L. T.; White, V.; Petrocelli, F.; Chadwick, D. Sour compression process for the removal of SOx and NOx from oxyfuel-derived CO2. *Energy Procedia*. **2011**, *4*, 908-916. https://doi.org/10.1016/j.egypro.2011.01.136.

(9) van der Lans, R. P.; Glarborg, P.; Dam-Johansen, K. Influences of process parameters on nitrogen oxide formation in pulverised coal burners. *Prog. Energy Combust. Sci*. **1997**, *23* (4), 349-377. https://doi.org/10.1016/S0360-1285(97)00012-9.

(10) Fenimore, C.P. Formation of nitric oxide in premixed hydrocarbon flames. *Symp. (Int.) Combust*. **1971**, *13* (1), 373-380. https://doi.org/10.1016/S0082-0784(71)80040-1.

(11) Okazaki, K.; Ando, T. NOx reduction mechanism in coal combustion with recycled CO2. *Energy*. **1997**, *22* (2-3), 207-215. https://doi.org/10.1016/S0360-5442(96)00133-8.

(12) Chan, L. K.; Sarofim, A. F.; Beer, J. M. Kinetics of the NO-carbon reaction at fluidized bed combustor conditions. *Combust. Flame.* **1983**, *52*, 37-45. https://doi.org/10.1016/0010-2180(83)90119-0.

(13) Andersson, K.; Normann, F.; Johnsson, F.; Leckner, B. NO emission during oxy-fuel combustion of lignite. *Ind. Eng. Chem. Res*. **2008**, *47* (6), 1835-1845. https://doi.org/10.1021/ie0711832.

(14) Normann, F.; Andersson, K.; Leckner, B.; Johnsson, F. High-temperature reduction of nitrogen oxides in oxy-fuel combustion. *Fuel*. **2008**, *87* (17-18), 3579-3585. https://doi.org/10.1016/j.fuel.2008.06.013.

(15) Ndibe, C.; Spörl, R.; Maier, J.; Scheffknecht, G. Experimental study of NO and NO2 formation in a PF oxy-fuel firing system. *Fuel*. **2013**, *107*, 749-756. https://doi.org/10.1016/j.fuel.2013.01.055.

(16) Hjärtsam, S.; Andersson, K.; Johnsson, F.; Leckner, B. Combustion characteristics of lignite-fired oxy-fuel flames. *Fuel*. **2009**, *88* (11), 2216-2224. https://doi.org/10.1016/j.fuel.2009.05.011.

(17) Stadler, H.; Christ, D.; Habermehl, M.; Heil, P.; Kellermann, A.; Ohliger, A.; Toporov, D.; Kneer, R. Experimental investigation of NOx emissions in oxycoal combustion. *Fuel*. **2011**, *90* (4), 1604-1611. https://doi.org/10.1016/j.fuel.2010.11.026.

(18) Mackrory, A. J.; Tree, D. R. Measurement of nitrogen evolution in a staged oxy-combustion coal flame. *Fuel*. **2012**, *93*, 298-304. https://doi.org/10.1016/j.fuel.2011.10.039.

(19) Watanabe, H.; Yamamoto, J.; Okazaki, K. NOx formation and reduction mechanisms in staged O2/CO2 combustion. *Combust. Flame.* **2011**, *158* (7), 1255-1263. https://doi.org/10.1016/j.combustflame.2010.11.006.

(20) Ma, H.; Zhou, L.; Ma, S.; Du, H. Design of porous wall air coupling with air staged furnace for preventing high temperature corrosion and reducing NOx emissions. *Appl. Therm. Eng*. **2017**, *124*, 865-870. https://doi.org/10.1016/j.applthermaleng.2017.06.029.

(21) Normann, F.; Andersson, K.; Leckner, B.; Johnsson, F. Emission control of nitrogen oxides in the oxy-fuel process. *Prog. Energy Combust. Sci*. **2009**, *35*, 385-397. https://doi.org/10.1016/j.pecs.2009.04.002.

(22) Zanganeh, K. E.; Shafeen, A. A novel process integration, optimization and design approach for large-scale implementation of oxy-fired coal power plants with CO2 capture. *Int. J. Greenhouse Gas Control*. **2007**, *1* (1), 47-54. https://doi.org/10.1016/S1750-5836(07)00035-7.

(23) Khare, S. P.; Wall, T. F.; Farida, A. Z.; Liu, Y.; Moghtaderi, B.; Gupta, R. P. Factors influencing the ignition of flames from air-fired swirl pf burners retrofitted to oxy-fuel. *Fuel*. **2008**, *87* (7), 1042-1049. https://doi.org/10.1016/j.fuel.2007.06.026.

(24) Chui, E. H.; Douglas, M. A.; Tan, Y. Modeling of oxy-fuel combustion for a western Canadian sub-bituminous coal. *Fuel*. **2003**, *82* (10), 1201-1210. https://doi.org/10.1016/S0016-2361(02)00400-3.

(25) Chui, E. H.; Majeski, A. J.; Douglas, M. A.; Tan, Y.; Thambimuthu, K. V. Numerical investigation of oxy-coal combustion to evaluate burner and combustor design concepts. *Energy*. **2004**, *29* (9-10), 1285-1296. https://doi.org/10.1016/j.energy.2004.03.102.

(26) Fry, A.; Adams, B.; Paschedag, A.; Kazalski, P.; Carney, C.; Oryshchyn, D.; Woodside, R.; Gerdemann, S.; Ochs, T. Principles for retrofitting coal burners for oxy-combustion. *Int. J. Greenhouse Gas Control.* **2011**, 5 (S1), S151-S158. https://doi.org/10.1016/j.ijggc.2011.05.004.

(27) Correa da Silva, R.; Kangwanpongpan, T.; Krautz, H. J. Flame pattern, temperatures and stability limits of pulverized oxy-coal combustion. *Fuel*. **2014**, 115, 507-520. https://doi.org/10.1016/j.fuel.2013.07.049.

(28) Hees, J.; Zabrodiec, D.; Massmeyer, A.; Pielsticker, S.; Govert, B.; Habermehl, M.; Hatzfeld, O.; Kneer, R. Detailed analyzes of pulverized coal swirl flames in oxy-fuel atmospheres. *Combust. Flame.* **2016**, *172*, 289-301. https://doi.org/10.1016/j.combustflame.2016.07.028.

(29) Correa da Silva, R.; Krautz, H. J. Emission performance of type-1 pulverized coal flames operating under oxy-fired conditions. *Appl. Therm. Eng.* **2014**, *64* (1-2), 430-440. https://doi.org/10.1016/j.applthermaleng.2013.12.065.

(30) Correa da Silva, R.; Krautz, H. J. Combustion measurements of type-1 pulverized coal flames operating under oxy-fired conditions. *Fuel Process. Technol*. **2018**, *171*, 232-247. https://doi.org/10.1016/j.fuproc.2017.10.014.

(31) Szuhánszki, J.; Farias Moguel, O.; Finney, K.; Akram, M.; Pourkashanian, M. Biomass combustion under oxy-fuel and post combustion capture conditions at the PACT 250 kW air/oxy-fuel CTF, http://www.supergen-bioenergy.net/media/eps/supergen/presentations/assembly-2017/25.10.2017_SUPERGEN---Sheffield-Project-outputs_for-web.pdf; 2017 [accessed 12 October 2018].

(32) Clements, A. G.; Black, S.; Szuhánszki, J.; Stechly, K.; Pranzitelli, A.; Nimmo, W.; Pourkashanian, M. LES and RANS of air and oxy-coal combustion in a pilot-scale facility:

Predictions of radiative heat transfer. *Fuel.* **2015**, *151*, 146-155. https://doi.org/10.1016/j.fuel.2015.01.089.

(33) Farias Moguel, O.; Szuhánszki, J.; Clements, A. G.; Ingham, D. B.; Ma, L.; Pourkashanian, M. Oscillating coal and biomass flames: A spectral and digital imaging approach for air and oxyfuel conditions. *Fuel Process. Technol*. **2018**, *173*, 243-252. https://doi.org/10.1016/j.fuproc.2018.02.002.

(34) Gharebaghi, M.; Irons, R .M. A.; Ma, L.; Pourkashanian, M.; Pranzitelli, A. Large eddy simulation of oxy-coal combustion in an industrial combustion test facility. *Int. J. Greenhouse Gas Control*. **2011**, *5* (S1), S100-10. https://doi.org/10.1016/j.ijggc.2011.05.030.

(35) Buhre, B. J. P.; Elliott, L. K.; Sheng, C. D.; Gupta, R. P.; Wall, T. F. Oxy-fuel combustion technology for coal-fired power generation. *Prog. Energy Combust. Sci*. **2005**, *31*, 283-307. https://doi.org/10.1016/j.pecs.2005.07.001.

(36) Woycenko, D. M.; van de Kamp, W. L.; Roberts, P.A. Combustion of pulverised coal in a mixture of oxygen and recycled flue gas. Summary of the APG research program, IFRF Doc. F98/Y/4. Ijmuiden, The Netherlands: International Flame Research Foundation (IFRF); October 1995.

(37) Levy, J. M.; Chan, L. K.; Sarofim, A. F.; Beer, J. M. NO/char reactions at pulverised coal flame conditions. *Symp. (Int.) Combust*. **1981**, *18* (1), 111-120. https://doi.org/10.1016/S0082-0784(81)80016-1.

(38) Mackrory, A. J.; Tree, D. R. Predictions of NOx in a laboratory pulverized coal combustor operating under air and oxy-fuel conditions. *Combust. Sci. Technol*. **2009**, *181* (11), 1413-30. https://doi.org/10.1080/00102200903373457.

(39) Kambara, S.; Takarada, T.; Yamamoto, Y.; Kato, K. Relation between functional forms of coal nitrogen and formation of NOx precursors during rapid pyrolysis. *Energy Fuels*. **1993**, *7* (6), 1013-1020. https://doi.org/10.1021/ef00042a045.

(40) Spinti, J. P.; Pershing, D. W. The fate of char-N at pulverized coal conditions. *Combust. Flame*. **2003**, *135* (3), 299-313. https://doi.org/10.1016/S0010-2180(03)00168-8.

(41) Shaddix, C. R.; Molina, A. Fundamental investigation of NOx formation during oxy-fuel combustion of pulverized coal. *Proc. Combust. Inst.* **2011**, *33* (2), 1723-1730. https://doi.org/10.1016/j.proci.2010.07.072.

(42) Pedersen, L. S.; Breithaupt, P.; Dam-Johansen, K.; Weber, R. Residence time in confined swirling flames. *Combust. Sci. Technol*. **1997**, *127* (1-6), 251-73. https://doi.org/10.1080/00102209708935696.